

Original Article

Intraperitoneal delivery of a novel liposome-encapsulated paclitaxel redirects metabolic reprogramming and effectively inhibits cancer stem cells in Taxol[®]-resistant ovarian cancer

Yao-An Shen^{1,2*}, Wai-Hou Li^{1*}, Po-Hung Chen¹, Chun-Lin He¹, Yen-Hou Chang^{1,2}, Chi-Mu Chuang^{1,3}

¹Section of Gynecologic Oncology, Department of Obstetrics and Gynecology, Taipei Veterans General Hospital, Taipei, Taiwan; ²Institute of Biochemistry and Molecular Biology, School of Life Sciences, National Yang-Ming University, Taipei, Taiwan; ³Institute of Clinical Medicine, School of Medicine, National Yang-Ming University, Taipei, Taiwan. *Equal contributors.

Received March 12, 2015; Accepted May 14, 2015; Epub May 15, 2015; Published May 30, 2015

Abstract: Taxol[®] remained as the mainstay therapeutic agent in the treatment of ovarian cancer, however recurrence rate is still high. Cancer stem cells (CSCs) represent a subset of cells in the bulk of tumors and play a central role in inducing drug resistance and recurrence. Furthermore, cancer metabolism has been an area under intensive investigation, since accumulating evidence has shown that CSCs and cancer metabolism are closely linked, an effect named as metabolic reprogramming. In this work, we aimed to investigate the impacts of a novel liposome-encapsulated paclitaxel (Nano-Taxol) on the stemness phenotype and metabolic reprogramming. A paclitaxel-resistant cell line (TR) was established at first. Tumor growth was induced in the mice peritoneal cavity by inoculation of TR cells. A 2x2 factorial experiment was designed to test the therapeutic efficacy in which factor 1 represented the comparison of drugs (Taxol[®] versus Nano-Taxol), while factor 2 represented the delivery route (intravenous versus intraperitoneal delivery). In this work, we found that intraperitoneal delivery of Nano-Taxol redirects metabolic reprogramming, from glycolysis to oxidative phosphorylation, and effectively suppresses cancer stem cells. Also, intraperitoneal delivery of Nano-Taxol led to a significantly better control of tumor growth compared with intravenous delivery of Taxol[®] (current standard treatment). This translational research may serve as a novel pathway for the drug development of nanomedicine. In the future, this treatment modality may be extended to treat several relevant cancers that have been proved to be suitable for the loco-regional delivery of therapeutic agents, including colon cancer, gastric cancer, and pancreatic cancer.

Keywords: Cancer stem cell, liposome, p53, stemness, epithelial-mesenchymal transition, metabolic reprogramming

Introduction

Conventional anti-cancer therapies typically target the rapidly dividing tumor cells, however, some tumor cells in the tumor microenvironment are spared. These spared tumor cells exhibit the potential to self-renewal and are called cancer stem cells (CSCs) [1, 2]. This may explain the clinical scenario in which a tumor has an apparent volumetric reduction after standard treatment, however, is subsequently followed by tumor recurrence. While debate continues as to the precise identity and function of CSCs, there is general agreement that

CSCs play a central role in the induction of drug resistance and tumor recurrence [3].

Cell proliferation involves the replication of all cellular contents with the required energy for this to happen. In normal cells, glucose participates in cellular energy production through its complete catabolism via the tricarboxylic acid (TCA) cycle and oxidative phosphorylation (OXPHOS). In solid tumors, the adaptation of CSCs in a relatively hypoxic environment resulting in a shift from OXPHOS to glycolysis has been elucidated. This shift has been termed as metabolic reprogramming [4, 5]. In the process

Nano-Taxol can switch status of cancer metabolism

of metabolic reprogramming, the glycolytic pathway is favored over OXPHOS as the primary form of bioenergetic metabolism even in the presence of oxygen, a feature first recognized by Otto Warburg as early as the 1920s [6]. Further, it is known that the CSCs exhibit different metabolism as compared to their more differentiated counterparts. Accumulating evidence has shown that CSCs demonstrate low quantity of mitochondrial DNA, high mitochondria membrane potential, low oxygen and glucose consumption, and a low intracellular concentration of adenosine triphosphate (ATP) and reactive oxygen species (ROS) as compared to the bulk of tumors [7]. In line with this, our group has also found that nasopharyngeal CSCs demonstrate different metabolism as compared to their differentiated counterparts, with greater reliance on glycolysis for energy supply and peri-nuclear distribution of mitochondria resembling those seen in normal stem cells [8].

Recent advances in nanotechnology have permitted the incorporation of multiple therapeutic, sensing and targeting agents into nanoparticles (for example, liposomes, viruses, and quantum dots), with a particle size ranges of 1-1,000 nm. These agents have offered new hope for detection, prevention, and treatment in oncology [9]. The enhanced permeability and retention (EPR) effect is now becoming the gold standard for the development of nanomedicine. All nanoparticles-based drugs use the EPR effect as a guiding principle for the drug development [10]. In theory, the use of nanoparticles should take the pharmacokinetic advantage by decreased clearance of the encapsulated drugs [11].

Ovarian cancer is the seventh most common cancer in women, with approximately 239,000 new cases and 140,200 estimated deaths worldwide [12]. In the United States, it is estimated that 21,980 women will be diagnosed with and 14,270 women will die of ovarian cancer in 2014 [13]. Ovarian cancer is essentially an intraperitoneal disease with tumor cells primarily disseminate along the peritoneum. Histology of peritoneum is basically a three-dimensional structure, which consists of a monolayer of mesothelial cells supported by a basement membrane and five layers of connective tissue which account for a total thickness of 90 μm , forming the so-called peritoneal-plasma barrier. Because of this peritoneal-plasma

barrier, intraperitoneal delivery of anti-cancer agents may take the pharmacokinetic advantage of getting drug levels that are 20 to 1000 times higher in the intraperitoneal cavity than in plasma [14].

In this translational research, we aimed to analyze an investigational drug: liposome-encapsulated paclitaxel (Nano-Taxol), which was compared with Taxol[®], a current standard drug in the treatment of ovarian cancer, with respect to stemness expression, cancer metabolism, and therapeutic efficacy. Delivery route is by either intravenous or intraperitoneal. The results of our work showed that intraperitoneal delivery of Nano-Taxol confers significantly better suppression of stemness signal and reversal of metabolic reprogramming than any other treatment modality. Moreover, reactivation of p53 was found to a critical factor in inducing these molecular changes. In line with these findings, intraperitoneal delivery of Nano-Taxol produced a dramatic anti-tumor efficacy, leading to prolonged survival of mice tested. The results of this translational research may be applied to a broad spectrum of tumors (e.g., colon cancer, gastric cancer, and pancreatic cancer) that are already proved to be suitable for loco-regional therapy.

Materials and methods

Cell culture

The human ovarian cancer cell line ES-2-luc (generously provided by the T.C. Wu lab at Johns Hopkins University) was used in the current work. ES-2-luc was cultured in complete Dulbecco's Modified Eagle Medium (DMEM), furnished with 1% sodium pyruvate; 1% non-essential amino acids; 1% antibiotics with penicillin and streptomycin sulphate; and 10% foetal bovine serum (FBS) (all purchased from Invitrogen, Carlsbad, CA) in a humidified incubator at 37°C with 5% CO₂. In this study, ES-2-luc was used as a parental cell line for the establishment of a derived paclitaxel-resistant cell line.

Establishment of chemo-resistant cell line and animal model

A Taxol[®]-resistant cell line was established from the parental ES-2-luc cells. Briefly, Taxol[®]-resistant clones were selected after ten rounds of Taxol[®] treatment (90% lethal dose each round and remaining 10% survival cells were

Nano-Taxol can switch status of cancer metabolism

Table 1. Primer sequences used in real-time RT-PCR analysis

Gene	Primer	Sequence (5' to 3')
18S rRNA	Forward	5-CTCAACACGGGAAACCTCAC-3
	Reverse	5-CGCTCCACCAACTAAGAACG-3
Oct4	Forward	5-GTGGAGAGCAACTCCGATG-3
	Reverse	5-TGCTCCAGCTTCTCCTTCTC-3
Sox4	Forward	5-CGAGTGGAACTTTTGTGCGA-3
	Reverse	5-TGTGCAGCGCTCGCAG-3
Klf4	Forward	5-CCGCTCCATTACCAAGAGCT-3
	Reverse	5-ATCGTCTTCCCCTCTTTGGC-3
c-Myc	Forward	5-GGAACGAGCTAAAACGGAGCT-3
	Reverse	5-GGCCTTTTCATTGTTTTCCAAC-3
Nanog	Forward	5-ATTCAGGACAGCCCTGATTCTC-3
	Reverse	5-TTTTTGCGCACTCTTCTCTGC-3
Lin28	Forward	5-CCCCCAGTGGATGTCTTT-3
	Reverse	5-CCCTCCTTCAAGCTCCGG-3
β -Catenin	Forward	5-CCAGCCGACACCAAGAAG-3
	Reverse	5-CGAATCAATCCAACAGTAGCC-3
Bmi1	Forward	5-AAATGCTGGAGAAGTGGAAAG-3
	Reverse	5-CTGTGGATGAGGAGACTGC-3
STAT3	Forward	5-GCACAGATTGCCTGCATTG -3
	Reverse	5-CTGCTAATGACGTTATCCAGT-3
HIF1a	Forward	5-TTTTTCAAGCAGTAGGAATTGGA-3
	Reverse	5-GTGATGTAGTAGCTGCATGATCG-3
Twist	Forward	5-GGAGTCCGAGCTTACGAG-3
	Reverse	5-TCTGGAGGACCTGGTAGAGG-3
Snail	Forward	5-CCTCCGTGTCAGATGAGGAC-3
	Reverse	5-CCAGGCTGAGGTATTCCTTG-3
Slug	Forward	5-GGGGAGAAGCCTTTTTCTTG-3
	Reverse	5-TCCTCATGTTTGTGCAGGAG-3
Zeb1	Forward	5-ACTGCTGGGAGGATGACAGA-3
	Reverse	5-ATCCTGCTTCATCTGCCTGA-3
E-cadherin	Forward	5-TGCCAGAAAATGAAAAGG-3
	Reverse	5-GTGTATGTGGCAATGCGTTC-3
N-cadherin	Forward	5-ACAGTGGCCACCTACAAAGG-3
	Reverse	5-CCGAGATGGGGTTGATAATG-3
Vimentin	Forward	5-GAGAAGTTTCCGTTGAAGC-3
	Reverse	5-GCTTCCTGTAGGTGGCAATC-3
Fibronectin	Forward	5-CAGTGGGAGACCTCGAGAAG-3
	Reverse	5-TCCCTCGGAACATCAGAAAC-3
MDR-1	Forward	5-TGGCAAAGAAATAAAGCGACTGA-3
	Reverse	5-CAGGATGGGCTCCTGGG-3
MRP-1	Forward	5-GCTTCCTCTTGGTGATATTCG-3
	Reverse	5-GCAGTTCAACGCATAGTGG-3
ABCG2	Forward	5-CATGTACTGGCGAAGAATATTTGGT-3
	Reverse	5-CACGTGATTCTTCCACAAGCC
MnSOD	Forward	5-GCTGACGGCTGCATCTGTT-3
	Reverse	5-CCTGATTTGGACAAGCAGCAA-3
Catalase	Forward	5-CTCCGGAACAACAGCCTTC-3
	Reverse	5-ATAGAATGCCCGCACCTG-3

the subjects for next run of selection) and subsequently selected by a single colony method for isolating homogeneous Taxol[®]-resistant clones. Through ten rounds of drug-selection and single colony method, ovarian Taxol[®]-resistant cell line (RR) was stably established after ten-months of culture procedures. Drug resistance index was evaluated by comparing IC₅₀ between RR cells and the parental ES-2-luc cells.

To examine whether this Taxol[®]-resistant clone express cross-resistance to other chemotherapeutic agents, several drugs were also tested including cisplatin, gemcitabine, liposomal-doxorubicin, and topotecan.

Tumor generation following a single intraperitoneal injection of Taxol[®]-resistant cells at d0 into 5-week-old SCID mice (CB.17 SCID/SCID) was consistently detectable three weeks post-injection through abdominal distension secondary to malignant ascites production. The animals were purchased from the National Laboratory Animal Breeding and Research Centre of Taipei which maintained in the oncology animal facility of the Taipei Veterans General Hospital (Taipei, Taiwan). The animals were utilized in compliance with the institutional animal health-care regulations. All of the experimental procedures pertaining to animals were approved by the Institutional Animal Care and Use Committee. The ovarian tumor-bearing mice were euthanized at the endpoint, specifically upon the appearance of visible signs of distress, such as fur ruffling, hunched posture, rapid respiratory rate, reduced activity, and progressive ascites formation. The dosing schedule for each indicated treatment mode was based on the maximum tolerated dose (MTD) according to preliminary studies.

Cell surface marker analysis

Cells were stained with anti-CD44-FITC (BD Bioscience, San Jose, CA, USA), anti-CD24-PE (BD Biosciences), and anti-CD133-PE antibodies (Miltenyi Biotec, MACS, Bergisch Gladbach, Germany). Rat anti-mouse immunoglobulin G (IgG)-FITC and rat anti-mouse IgG-PE were utilized as isotype negative controls (BD Biosciences). The cells were then incubated on ice for 30 min and washed twice preceding analysis by a Cytomics FC500 Flow Cytometer (Beckman Coulter, Inc., Fullerton, CA, USA).

Nano-Taxol can switch status of cancer metabolism

Real-time RT-PCR analysis

Total RNA was extracted with the TRIsure™ reagent (Bioline Reagents Ltd, London, UK), and its concentration and purity were measured by a NanoDrop ND-1000 Spectrophotometer (NanoDrop Technologies, Inc., Wilmington, DE, USA). Real-time PCR was performed using the SensiFAST™ SYBR Hi-ROX Kit (Bioline) through an ABI StepOnePlus™ Real-Time PCR machine (Applied Biosystems, Foster City, CA, USA). The PCR primer sequences are listed in **Table 1**.

Antibodies for immunofluorescence staining

Antibodies against GLUT-1 (1:500, Abcam), phospho-p53 (Ser15) (1:500, Cell Signaling, Boston, MA), or CD44 (1:500, Abcam), were used for immunofluorescence staining.

Measurement of oxygen consumption rate and extracellular acidification rate

The oxygen consumption rate (OCR) and the extracellular acidification rate (ECAR) were determined by using a Seahorse XF-24 extracellular flux analyser. For the 30 min before the assay, the cells culture medium was replenished with un-buffered DMEM and incubated at 37°C to stabilize the pH and temperature. The OCR reflects the mitochondrial respiration rate, and the ECAR represents the rate of lactate production during glycolysis.

Glucose uptake assay

To measure the rate of glucose uptake, a fluorescent glucose analogue was used to monitor glucose uptake in live cells. Cells were cultured for 2 hr at 37°C in glucose-free medium containing 100 µM of 2-(N-(7-nitrobenz-2-oxa-1,3-diazol-4-yl)amino)-2-deoxyglucose (2-NBDG, Invitrogen). The fluorescence intensity of the 2-NBDG uptake was quantified by flow cytometry (Cytomics FC500, Beckman Coulter, Fullerton, CA), and the images were captured by an Olympus FV10i confocal microscope (Olympus America Inc., Center Valley, PA).

Measurement of mitochondrial mass

Cells were stained with a 2.5 µM nonyl acridine orange (NAO, Invitrogen) for 10 min at 25°C in the dark and then harvested in a solution containing 5 mM KCl, 140 mM NaCl, 2 mM CaCl₂, 1

mM MgCl₂, 10 mM glucose, and 5 mM HEPES buffer (pH 7.4). The fluorescence intensity was detected by flow cytometry (Cytomics FC500, Beckman Coulter).

Measurement of mitochondrial membrane potential ($\Delta\psi_m$)

Cells were incubated with 100 nM of the tetramethylrhodamine methyl ester (TMRM) fluorescent dye (Invitrogen) for 30 min at 37°C. The fluorescence intensity was monitored using a Cytomics FC500 flow cytometer (Beckman Coulter).

Measurement of reactive oxygen species (ROS) and antioxidants

Cells were incubated in DMEM containing 5 µM CellROX® Green Reagent (Invitrogen) or MitoSOX Red (Invitrogen) for 15 min at 37°C. CellROX Green was employed for the measurement of intracellular ROS, and MitoSOX Red was used to monitor the mitochondrial superoxide anions. The fluorescence intensities of CellROX Green and MitoSOX Red were analysed using a Cytomics FC500 flow cytometer (Beckman Coulter), and images were captured by an Olympus FV10i confocal microscope (Olympus America Inc.). For the evaluation of the cellular level of reduced glutathione (GSH), cells were incubated with 8 µg/mL VitaBright-48 solution (VB48; ChemoMetec A/S, Allerød, Denmark) for 5 min at 37°C. The fluorescence intensity of VB48 was measured using a 405-nm laser excitation wavelength and a 475/25-nm emission wavelength by an Olympus FV10i confocal microscope (Olympus America Inc.).

Statistical analysis

All data are presented as the mean ± SD. Statistical analysis was performed using Student's *t*-test for continuous variables. Survival between each indicated group are analysed by log-rank test. *p* < 0.05 was considered statistically significant.

Results

Taxol®-resistant cells express stemness and epithelial-to-mesenchymal transition phenotype

Clonogenic assay of both Taxol®-resistant cells and the parental cells was shown, with drug

Nano-Taxol can switch status of cancer metabolism

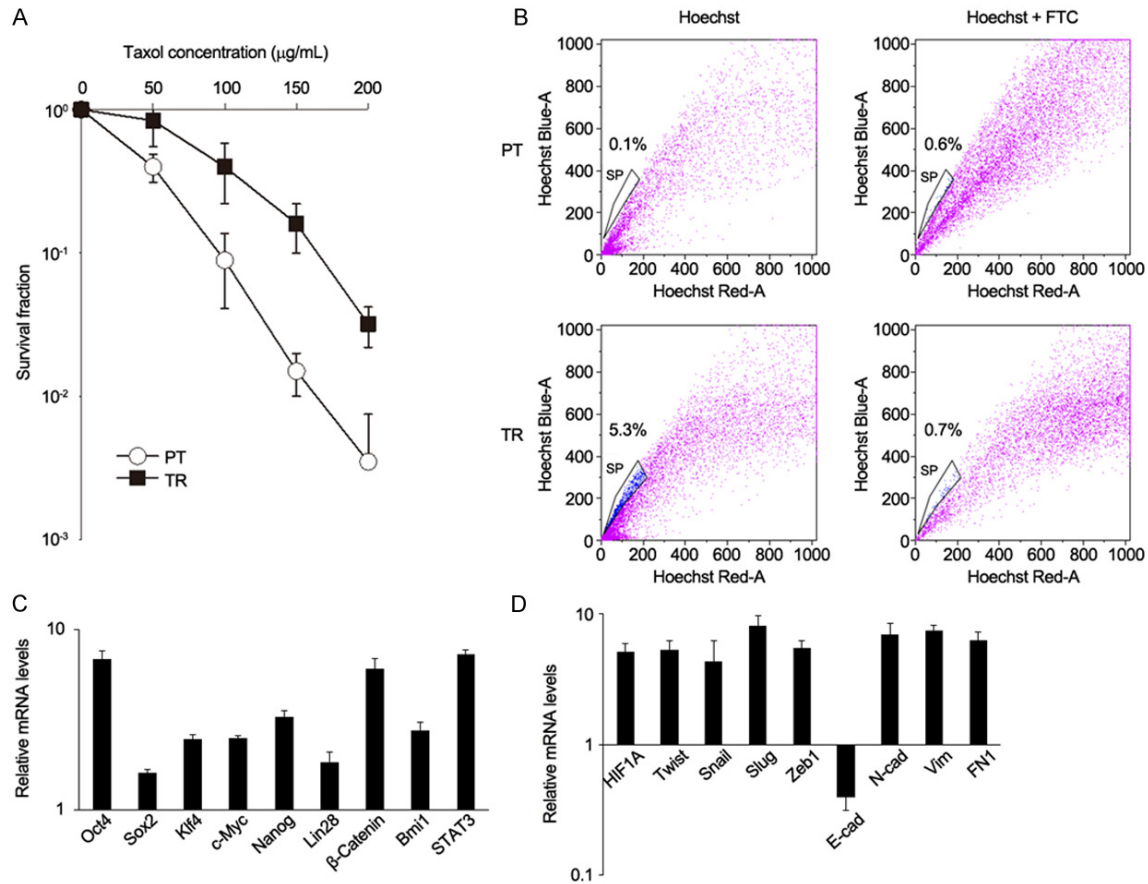


Figure 1. Paclitaxel-resistant ovarian cancer cells exhibit a radiation-resistance phenotype with expression of stemness and epithelial-mesenchymal transition markers. **A.** Survival fractions of ES-2 paclitaxel-resistant cells (TR) and parental ES-2-luc cells (PT). Chemo-resistant cells exhibited significantly higher survival fraction than the parental cells under various doses of irradiation. **B.** Percentage of side population is elevated in ES-2 chemo-resistant cells compared to ES-2-luc parental cells. **C.** TR cells expressed elevated stemness-associated gene expression levels compared with PT cells. Data were normalized to 18S mRNA levels and compared with those of parental cells. **D.** TR cells expressed elevated levels of the EMT regulator genes, such as *HIF1a*, *Twist*, *Snail*, *Slug*, *Zeb1*, and of the mesenchymal markers *N-cadherin*, *Vimentin*, and *Fibronectin*, whilst the epithelial marker *E-cadherin* was decreased. Data were normalized against 18S mRNA levels and compared with those of parental cells. Results are presented as the mean \pm SD for triplicate experiments (**, $P < 0.01$).

resistance index = 3.4 by comparing IC_{50} (Figure 1A). The percentage of CSC-like side population was increased in Taxol[®]-resistant cells (Figure 1B). Next, we compared the expression of stemness-associated markers and transcription factors (*Oct4*, *Sox2*, *Klf4*, *c-Myc*, *Nanog*, *Lin28*, β -catenin, *Bmi1*, *STAT3*) of Taxol[®]-resistant cells with the parental cells by qRT-PCR analysis. As shown, these molecules were all increased (Figure 1C). Taxol[®]-resistant cells also manifested features of EMT with decrease of the epithelial marker *E-cadherin* and concomitantly with increase of the mesenchymal markers *N-cadherin*, *Vimentin* and *Fibronectin*, as well as of the EMT-related transcription factors *HIF1 α* , *Twist*, *Snail*,

Slug, and *Zeb1* (Figure 1D). In summary, Taxol[®]-resistant cells exhibited CSCs-like behavior with drug resistance index of 3.4.

Taxol[®]-resistant cells display metabolic hallmarks similar to cancer stem cells

Taxol[®]-resistant cells underwent the process of metabolic reprogramming pertaining to a metabolic shift and mitochondrial resetting. Through metabolic shift, Taxol[®]-resistant cells manifested faster glucose uptake and a higher expression level of the glucose transporter GLUT1 than the parental cells (Figure 2A). Further, Taxol[®]-resistant cells demonstrated mitochondrial resetting with an increased level of antioxi-

Nano-Taxol can switch status of cancer metabolism

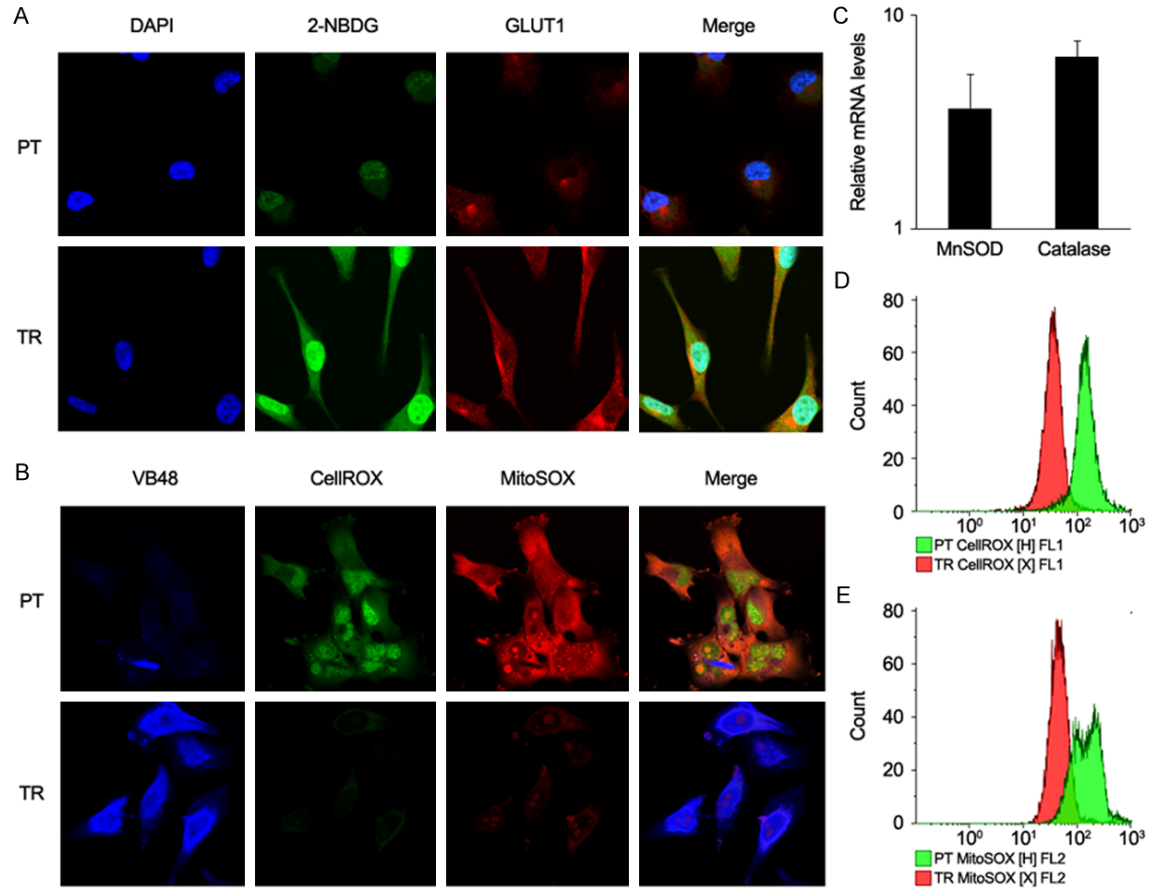


Figure 2. Chemo-resistant ovarian cancer cells display a glycolytic metabolism. (A) Immunofluorescence staining of 2-NBDG uptake and GLUT1 expression captured by confocal microscopy indicating the augmented levels of glucose uptake in TR cells compared with PT cells. 2-NBDG is a fluorescent glucose analogue for monitoring the rate of glucose uptake. (B) TR cells upregulated antioxidants, such as reduced glutathione (GSH), resulting in lower levels of intracellular ROS and mitochondrial superoxide anions compared with parental cells. VB48, CellROX Green and MitoSOX were utilized for measuring the levels of reduced glutathione, intracellular ROS, and mitochondrial superoxide anions, respectively. (C) TR cells manifested higher levels of the antioxidants MnSOD and Glutathione than PT cells. Data were normalized against 18S mRNA expression levels and compared with those of PT cells. (D-E) Flow cytometry depicted that (D) intracellular ROS and (E) mitochondrial superoxide anions levels were comparatively lower in TR cells compared to PT cells. Data are presented as mean \pm SD for triplicate experiments.

dants, including reduced glutathione (GSH) (**Figure 2B**), MnSOD and catalase (**Figure 2C**), resulting in scavenging of intracellular ROS and mitochondrial superoxide anions, which were distinctly different from their parental cells (**Figures 2B, 2D** and **2E**). These observations disclosed that Taxol[®]-resistant cells exhibit metabolic characteristics similar to CSCs.

Intraperitoneal delivery of Nano-Taxol can effectively suppress CSCs-like subpopulation with redirection of tumor metabolism back to OXPHOS

To explore which delivery route offers the best CSCs-killing effect, we established an ortho-

topic xenograft model by inoculating Taxol[®]-resistant cells into ovarian tissues. After indicated treatment, tumor cells were then retrieved for further experiments. By comparing intravenous or intraperitoneal delivery of Taxol[®] or Nano-Taxol, we found that intraperitoneal delivery of Nano-Taxol significantly suppressed CSCs-like subpopulation as shown by the diminished quantities of CD44, CD24, and CD133 expressing cells (**Figure 3A-C**). Next, we measured the oxygen consumption rate (OCR) and extracellular acid efflux rate (ECAR) via a Seahorse XF24 extracellular Flux analyser. OCR represents mitochondrial respiration, while ECAR is an indicator of the lactic acid produc-

Nano-Taxol can switch status of cancer metabolism

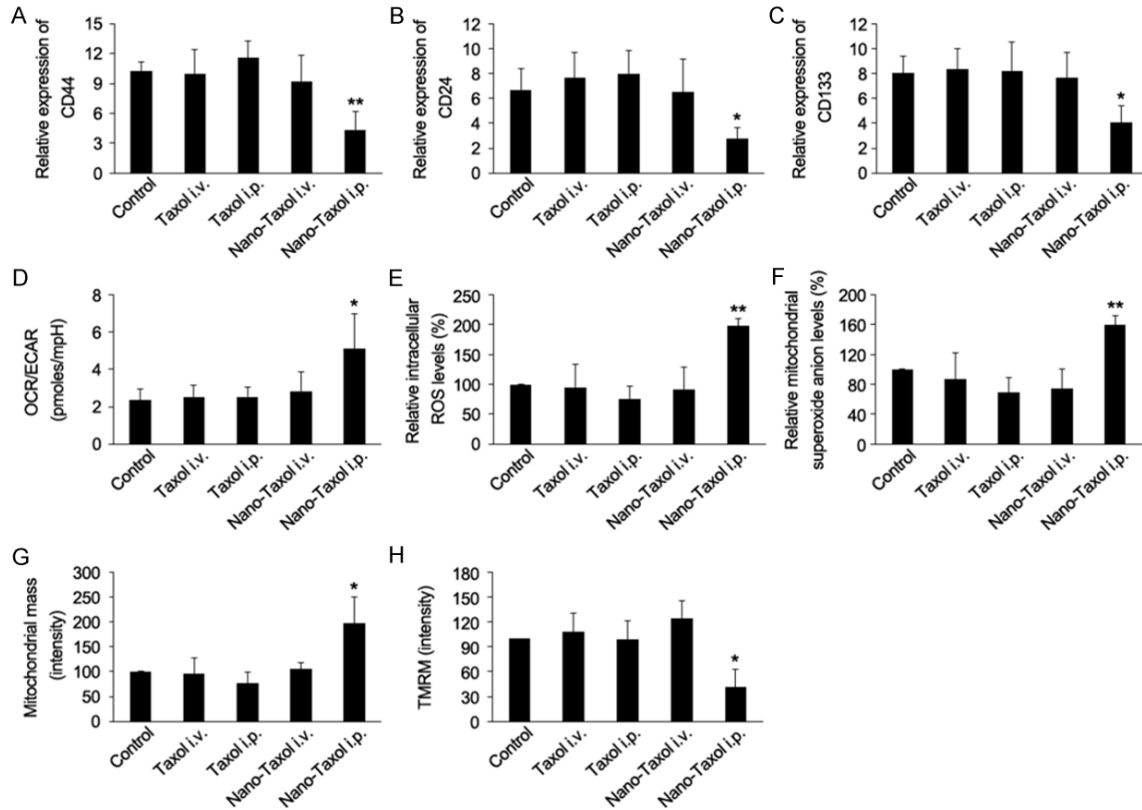


Figure 3. Intraperitoneal delivery of Nano-Taxol can decrease the expression of stemness markers and redirect metabolism towards OXPHOS. (A-C) Intraperitoneal Nano-Taxol delivery eradicated the CSCs-like subpopulation, as shown by the reduced number of cells expressing (A) CD44, (B) CD24, and (C) CD133 as quantified by flow cytometry. Tumor cells were harvested following inoculation of TR cells for each indicated group. Dosing schedules were detailed in materials and methods. (D) Intraperitoneal Nano-Taxol delivery significantly increased the OCR/ECAR ratio, as analysed by a Seahorse analyser. (E-F) Intraperitoneal Nano-Taxol delivery prominently increased the (E) intracellular levels of ROS and (F) mitochondrial superoxide anions. CellROX Green was used for monitoring intracellular ROS, and MitoSOX was used for measuring mitochondrial superoxide anions levels as quantified by flow cytometry. (G) Intraperitoneal delivery of Nano-Taxol delivery increased the mitochondrial mass, as measured by NAO staining followed by flow cytometry. (H) TMRM staining measured by flow cytometry, indicates the depolarization of the mitochondrial membrane potential in the group treated with intraperitoneal Nano-Taxol delivery. Data are presented as the mean \pm SD for triplicate experiments (*, $P < 0.05$; **, $P < 0.01$).

tion rate during glycolysis. Intraperitoneal delivery of Nano-Taxol demonstrated increased OCR/ECAR ratio (**Figure 3D**), increased intracellular ROS levels (**Figure 3E**), increased mitochondrial superoxide anion levels (**Figure 3F**), elevated mitochondrial mass (**Figure 3G**), and depolarized the mitochondrial membrane potential (**Figure 3H**), indicating that this treatment can redirect metabolic reprogramming, switching glycolysis to OXPHOS. Taken together, intraperitoneal delivery of Nano-Taxol demonstrated a promising avenue towards the efficient elimination of the CSCs-like subpopulation within the tumor mass, resulting in the switch of the CSCs metabolic hallmark from a glycolytic metabolism to OXPHOS.

Intraperitoneal delivery of Nano-Taxol delivery suppresses CSCs-like subpopulation and redirects metabolic reprogramming through reactivation of p53

Growing evidence has shown that the pharmacological reactivation of p53 function can exert a profound suppression of several types of tumors, such as lymphomas, soft tissue sarcomas and hepatocellular carcinomas, without affecting normal tissues [15, 16]. In this work, p53 was remarkably activated in Taxol[®]-resistant cells after treatment with Nano-Taxol by *in vitro* assay (third row panel in **Figure 4A**), whereas this phenomenon was not seen with Taxol[®] treatment (second row panel in **Figure 4A**).

Nano-Taxol can switch status of cancer metabolism

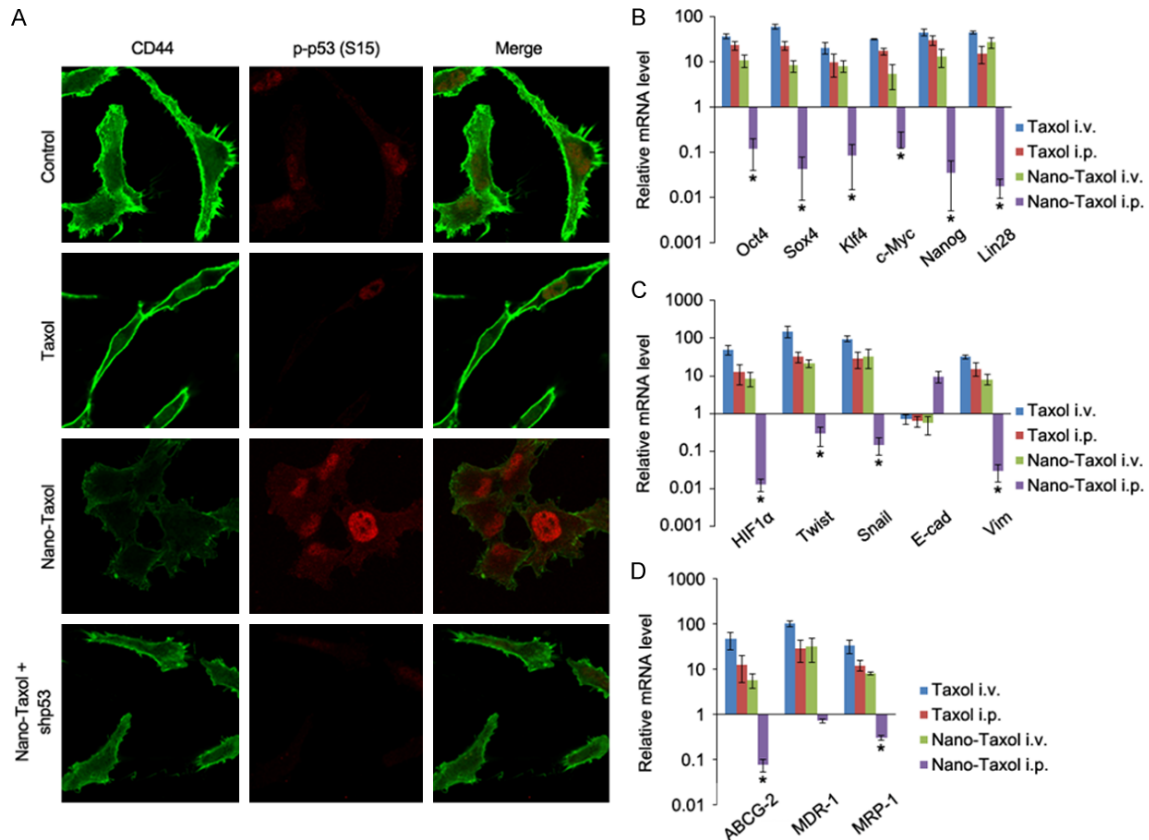


Figure 4. Activation of p53 reveals a critical role in suppressing epithelial-to-mesenchymal transition. (A) Immunofluorescence staining demonstrates that the Nano-Taxol significantly activated p53 expression (active form indicated by phosphorylation on Ser15) in TR cells. (B-D) qRT-PCR analysis: (B) Intraperitoneal Nano-Taxol treatment reduced the stemness related genes in tumors originated from TR cells extracted from SCID mice. (C) Intraperitoneal Nano-Taxol treatment redirected the EMT process, as supported by the upregulation of *E-cadherin* (*E-cad*) expression and the downregulation of *HIF1α*, *Twist*, *Snail*, *vimentin* (*Vim*) expression in TR tumors retrieved from SCID mice. (D) Intraperitoneal delivery of Nano-Taxol reduced the expression of drug resistant genes. Data in (B-D) were normalized with *18S mRNA* expression level and compared with expression in parental cells without the corresponding treatment with either paclitaxel or Nano-Taxol (*, $P < 0.05$).

To confirm whether Nano-Taxol could suppress the CSCs properties directly through the reactivation of a functional p53, we knocked down p53 expression in Nano-Taxol-treated tumor cells by transducing a lentivirus-based shRNA targeting p53. As shown, expression of stemness marker CD44 is significantly suppressed (fourth row panel of **Figure 4A**). We also found that intraperitoneal delivery of Nano-Taxol remarkably reduced the expression of stemness (**Figure 4B**) and EMT related genes (**Figure 4C**) in tumors originated from Taxol[®]-resistant cells. Also, drug resistant genes such as ABCG-2, MDR-1, and MRP-1 were down-regulated by this treatment modality (**Figure 4D**).

Next we investigated the impact of reactivation of p53 on metabolic reprogramming. As shown,

treatment with Nano-Taxol suppressed the expression of 2-NBDG (an indicator of glucose uptake) and GLUT1 (a glucose transporter), indicating that Nano-Taxol could suppress avid glucose intake (third row panel of **Figure 5A**). In contrast, treatment with Taxol[®] failed to show such phenomenon (second row panel of **Figure 5A**). In the group that treated with Nano-Taxol, p53 knockdown restored avid glucose uptake again (fourth row panel of **Figure 5A**).

Accordingly, treatment with Nano-Taxol increased the expression of CellROX (an indicator of cell stress) and MitoSOX (an indicator of mitochondrial superoxide production), indicating that Nano-Taxol could enhance tumor cell stress and mitochondrial superoxide production, leading to increased toxicities to tumor

Nano-Taxol can switch status of cancer metabolism

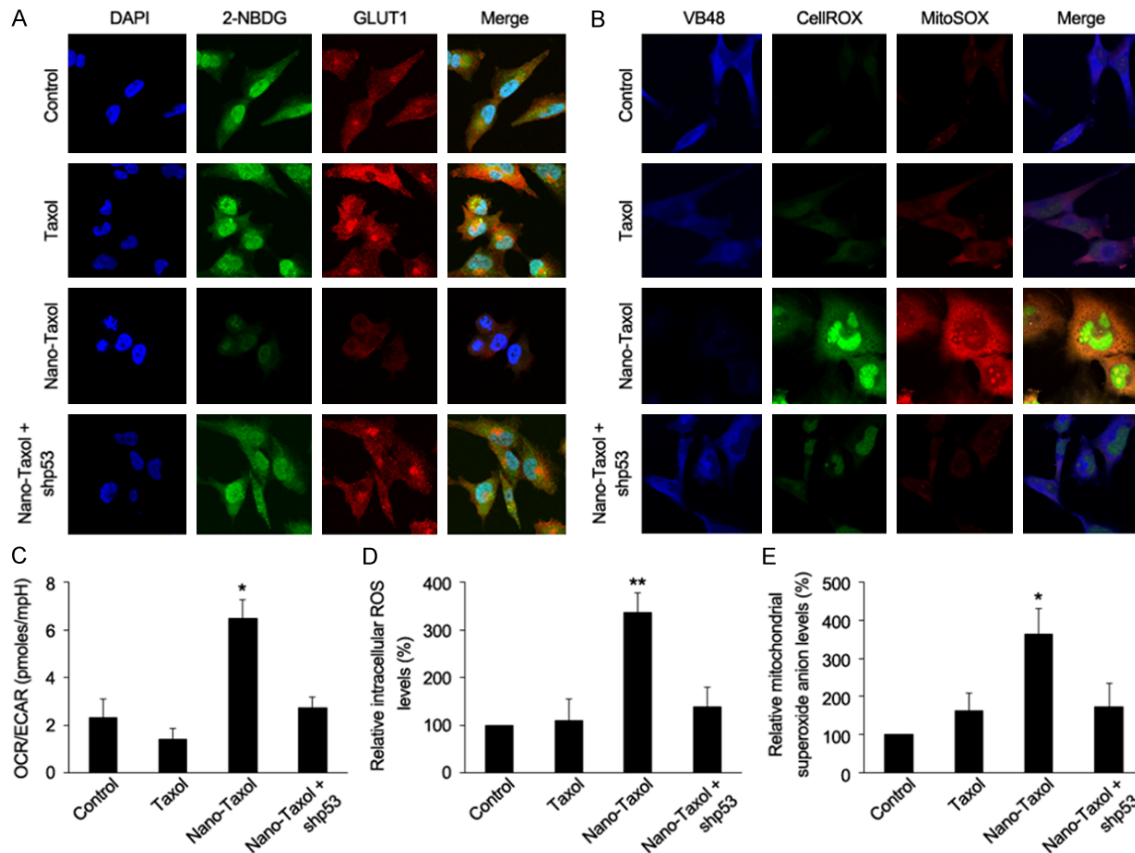


Figure 5. Nano-Taxol reactivates OXPHOS through induction of p53. A. Nano-Taxol treatment significantly suppressed the glucose uptake and expression of GLUT1 in TR cells, while p53 knockdown reversed these effects. Representative is shown. B. Nano-Taxol treatment attenuated glutathione (GSH) levels, which resulted in the accumulation of intracellular ROS and mitochondrial superoxide anions levels in TR cells. Knockdown of p53 reversed the effects of Nano-Taxol. Representative figure is shown. C. Increase of OCR/ECAR ratio reflects the switch from glycolysis to OXPHOS upon Nano-Taxol treatment in TR cells, while p53 knockdown abolished the effects exerted by Nano-Taxol. D. Summary of intracellular ROS levels for each indicated group. E. Summary of mitochondrial superoxide anions levels. p53 knockdown abolished the effects of Nano-Taxol. Data are presented as mean \pm SD for triplicate experiments (*, $P < 0.05$; **, $P < 0.01$).

cells (third row panel of **Figure 5B**). In contrast, treatment with Taxol[®] failed to show such phenomenon (second row panel of **Figure 5B**). In the group that treated with Nano-Taxol, p53 knockdown suppressed toxicities to tumor cells (fourth row panel of **Figure 5A**).

In line with afore-mentioned findings, treatment with Nano-Taxol increased the OCR/ECAR ratio (**Figure 5C**), relative intracellular ROS levels (**Figure 5D**), and mitochondrial superoxide levels (**Figure 5E**). In summary, these data support the contention that treatment with Nano-Taxol can redirect tumor metabolism, switching from glycolysis to OXPHOS, predominately driven through the induction of p53. These results substantiated the molecular pathway that Nano-Taxol blocks stemness traits and redi-

rects metabolic reprogramming in a p53-dependent manner.

Intraperitoneal delivery of Nano-Taxol confers better tumor control than the current standard therapy against ovarian cancer

To evaluate the therapeutic effect of Nano-Taxol *in vivo*, we orthotopically inoculated chemo-resistant cells into the ovarian tissue of SCID mice. At day 8 and day 10, we treated mice with 1/3 of the maximum tolerated dose (MTD) of Taxol[®] or Nano-Taxol, through either intravenous or intraperitoneal delivery. By *in vivo* imaging systems (IVIS) captured at 15 days after tumor inoculation, tumors were poorly controlled when treated with intravenous or intraperitoneal delivery of Taxol[®], and treated

Nano-Taxol can switch status of cancer metabolism

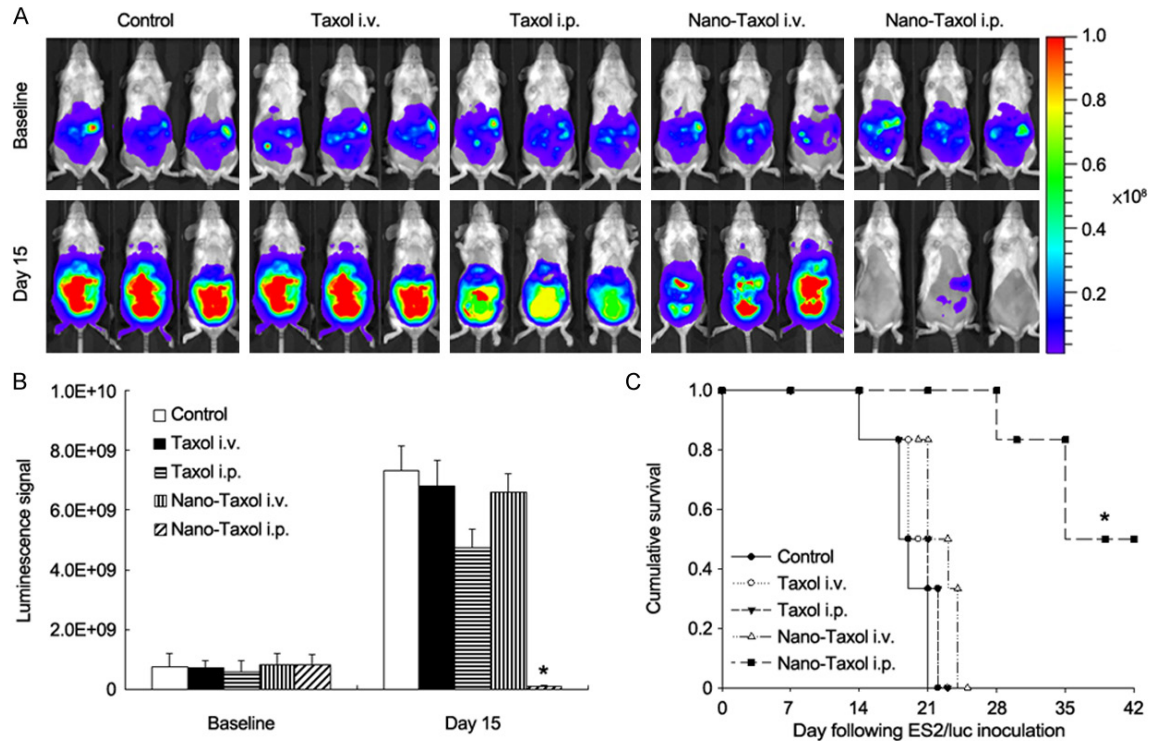


Figure 6. Intrapерitoneal Nano-Taxol delivery offers significant tumor-killing effects. (A) Tumors originating from Taxol[®]-resistant cells were detected at d 15 in the abdominal region of SCID mice using an *in vivo* bioluminescence imaging system (IVIS). Representative figures are shown from triplicate experiments. (B) Summary of quantitative luminescence signals of IVIS images in (A), indicating that intraperitoneal delivery of Nano-Taxol displayed remarkable tumor-killing effects. (C) Overall survival curve signifies that intraperitoneal Nano-Taxol delivery confers the longest survival time (*, $P < 0.05$, compared with other treatment groups by log-rank test).

with intravenous delivery of Nano-Taxol. In contrast, tumors were effectively eradicated when treated with intraperitoneal delivery of Nano-Taxol (Figure 6A and 6B). Moreover, intraperitoneal delivery of Nano-Taxol remarkably extended overall survival compared with other treatment groups (Figure 6C). Collectively, the aforementioned *in vitro* and *in vivo* data solidify that intraperitoneal delivery of Nano-Taxol, by providing a longer retention time in the peritoneal cavity due to the physical traits of nanoparticles, could potentially pave a novel therapeutic strategy against CSCs-containing ovarian tumors with inherent drug resistance capacity, by redirecting their metabolic reprogramming through the reactivation of p53 function.

Schematic illustration of the therapeutic effects resulting from intraperitoneal delivery of Nano-Taxol

Our work clearly elucidates that the intraperitoneal delivery of Nano-Taxol can effectively suppress the expression of stemness-associated

markers and reactivate p53. These effects can redirect the metabolic programming, switching from glycolysis to OXPHOS, and effectively control tumor growth (Figure 7A). In contrast, intraperitoneal or intravenous delivery of Taxol[®] and intravenous delivery of Nano-Taxol, failed to suppress the expression of stemness-associated markers and failed to redirect metabolic reprogramming, poorly control tumor growth (Figure 7B).

Discussion

The major finding in this work points out that intraperitoneal delivery of a novel anti-tumor drug: liposome-encapsulated paclitaxel (Nano-Taxol) can effectively suppress the expression of stemness markers and redirect metabolic reprogramming, switching from glycolysis back to OXPHOS status. Further, reactivation of p53 plays a central role in inducing these phenomena, and knock-down of p53 completely abolish these effects. Collectively, these molecular responses exert a dramatic anti-tumor thera-

Nano-Taxol can switch status of cancer metabolism

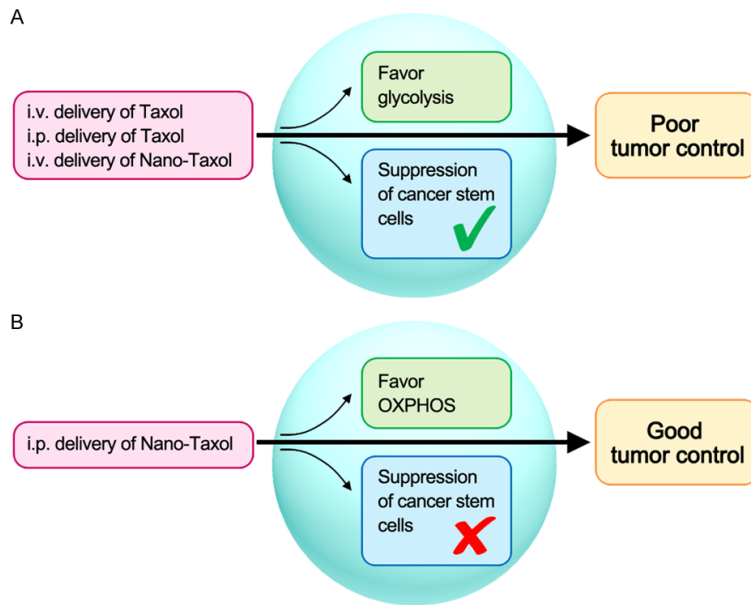


Figure 7. Schematic representation of the outcome following the intraperitoneal delivery of Nano-Taxol for the treatment of ovarian cancer. A. Intraperitoneal Nano-Taxol delivery can effectively suppress the expression of stemness-associated markers and redirect metabolic programming back to OXPHOS, resulting in a satisfactory control of tumor growth. B. In contrast, intraperitoneal and intravenous delivery of Taxol® or intravenous delivery of Nano-Taxol failed to suppress expression of stemness-associated markers and also failed to redirect metabolic reprogramming, resulting in poor tumor control.

peutic efficacy, as mice treated with intraperitoneal delivery of Nano-Taxol showed the longest survival compared with the other three treatment groups (intravenous delivery of Nano-Taxol, and either intravenous or intraperitoneal delivery of Taxol®). Currently, intravenous delivery of Taxol® remains the standard treatment for ovarian cancer, and notwithstanding an initial response may occur, about 75% patients of advanced disease will eventually face tumor recurrence [17]. Development of Nano-Taxol may overcome the current problem of Taxol®, conferring higher anti-tumor efficacy.

The experimental algorithm of our research design is as follows: First, we aimed to investigate whether an established Taxol®-resistant ovarian cancer cell line (TR cells) harbors higher expression of stemness markers and shows evidence of epithelial-mesenchymal transition, compared with the parental cell line (PT cells) (Figure 1). Second, we proved that TR cells displayed a pro-glycolytic phenotype, while PT cells showed an OXPHOS status (Figure 2). Third, we evaluated the expression of stem-

ness markers and cellular metabolism by different drugs (Taxol® or Nano-Taxol) and by different delivery route (intravenous or intraperitoneal). Among the different combination of treatment modalities, intraperitoneal delivery of Nano-Taxol exhibited the best suppression of stemness markers, and concomitant with reversal from pro-glycolytic metabolism to OXPHOS status (Figure 3). Fourth, we proved that activation of p53 plays a central role in driving the change of stemness expression and metabolism status. Knock-down of p53 by short hairpin RNA abolished these changes (Figures 4, 5). Lastly, we demonstrated that intraperitoneal delivery of Nano-Taxol conferred the best anti-tumor efficacy (Figure 6). A schematic presentation of treatment and molecular responses is shown in Figure 7.

Although our data show that intraperitoneal delivery of Nano-Taxol exhibits a dramatic anti-tumor efficacy, however, intravenous delivery of this new investigational drug failed to show efficacy. There are two putative reasons. First reason: the inherent limitations of EPR effect. In theory, nanoparticle-encapsulated therapeutic agent is supposed to accumulate within tumors due to the EPR effect and then release their therapeutic payloads in the tumor tissues. However, in reality, the EPR effects provide, at most, a relatively modest specificity offering about 20-30% increases in drug delivery [18]. Indeed, some nanoparticle-encapsulated agents have shown efficacy in animal models of cancer and several agents are under testing in clinical trials. However, response rates vary, likely related to the broad heterogeneity of EPR effects observed among tumor types and within individual tumors [19, 20]. Before the EPR effect can be effectively exploited in the field of nanomedicine, several factors have to be evaluated, including (i). The degree of angiogenesis and lymphangiogenesis. (ii). The degree of perivascular tumor growth adjacent to the vascula-

ture and the density of the stromal response. (iii). Intratumoral pressure [21]. Second reason: the existence of peritoneal-plasma barrier. Previous reports have suggested that systemic delivery of anticancer drugs has a limiting effect on peritoneal lesions due to the peritoneal-plasma barrier, which prevent the effective drug delivery from blood into the peritoneal cavity [22, 23]. As such, for an intraperitoneal disease, for example ovarian cancer, bypassing the EPR effect and the peritoneal-plasma barrier, by rerouting the payload by intraperitoneal delivery may directly solve this problem. As evidenced, our data show that intraperitoneal delivery of Nano-Taxol confers the best anti-tumor efficacy.

Our work also demonstrates that intraperitoneal delivery of Taxol[®], a current standard drug in the treatment of ovarian cancer, did show some anti-tumor efficacy (**Figure 6A**), as evidenced by decreased bioluminescence signal compared with intravenous delivery of Nano-Taxol or intravenous delivery of Taxol[®] (**Figure 6A and 6B**). In line with our finding, intraperitoneal delivery of Taxol[®] has been shown to be efficacious in clinical trials [24, 25]. However the *dose-limiting toxicity of Taxol[®] by intraperitoneal delivery*, was severe abdominal pain, likely caused by the excipients (Cremophor EL and *ethanol*) that are required to overcome low drug solubility [26]. As such, development of excipient-free paclitaxel may be warranted. The investigation new drug in the current work (Nano-Taxol) is excipient-free which may overcome the problem of abdominal pain.

Further, the lipid-based drug delivery systems have emerged as a highly suitable formulation strategy to increase the bioavailability of poorly water soluble drugs. These systems include many different type of drug delivery platform including oil solutions (e.g., liposomes in the current work), emulsions, microemulsions, self-emulsifying drug delivery systems and micellar systems. Such vehicles typically comprise a digestible lipid with (in the case of more complex self-emulsifying formulations) a blend of surfactants, co-surfactants and potentially co-solvents [27, 28]. We proved that intraperitoneal delivery of Nano-Taxol confers better anti-tumor efficacy than intraperitoneal delivery of Taxol[®], indicating that Nano-Taxol provides better bioavailability than Taxol[®].

Also, intraperitoneal delivery of Nano-Taxol can effectively suppress the expression of stemness markers and reverse the cellular metabolism status, from glycolysis to OXPHOS. Accumulating evidence has shown that CSCs display significant alternation of metabolism and are more pro-glycolytic compared with more differentiated tumor counterparts [29-31]. It has also been suggested that the strategy of targeting glycolysis can be exploited to develop new pharmacological agents that can counteract the treatment related resistance of CSCs [32]. Indeed, it has been shown that glycolytic inhibitor can effectively eliminate CSCs and consequently achieve desirable tumor control [33, 34].

We also found that reactivation of p53 function through intraperitoneal delivery of Nano-Taxol plays a central role in combating ovarian cancer. We found that reactivation of p53 function resulted in suppression of epithelial-mesenchymal transition and reversal of glycolysis. Accordingly, short hairpin RNA-mediated knock-down of p53 function abolished these effects (**Figures 4 and 5**). p53 is one of the most well-established tumor suppressor genes in the cancer research field [35]. In terms of cancer metabolism, p53 performs several intricate roles to attenuate the glycolytic pathway by upregulating p53-induced glycolysis and apoptosis regulator and phosphoglycerate mutase to down-regulate glycolytic enzymes and decreasing the expression of glucose transporter 1 (GLUT1) and GLUT4 [36-38]. Further, p53 can accelerate mitochondrial respiration by means of inducing synthesis of cytochrome c oxidase 2 and glutaminase 2 [39, 40]. As such, restoring the p53 function and its downstream targets is a potential therapeutic strategy for cancer treatment. It has been shown that pharmacological agents that restore the activities of p53 or mimicking the metabolic effect of p53, have practical applications for cancer treatment [41-43].

The results of the current work can be corroborated by the successful licensing of liposomal cytarabine (DepoCyt[®]), an approved nanomedicine for the treatment of leptomeningeal metastases of lymphoma or leukemia, by intrathecal delivery (a type of loco-regional delivery). In a randomized controlled trial, the intrathecal delivery of DepoCyt[®] was administered at lower

doses compared with free cytarabine, and nonetheless, DepoCyt® demonstrates an increased tumor response rate (71% vs. 15%) [44]. In fact, there exist two common points between Nano-Taxol and DepoCyt®: First, loco-regional delivery of these two therapeutic agents (intraperitoneal delivery for Nano-Taxol, while intrathecal delivery for Depocyt). Second, both agents are nanoparticles-encapsulated agents (liposomes for both Nano-Taxol and DepoCyt®). These two common points may provide some evidence for the pharmaceutical industry to consider developing nanoparticle-encapsulated agents through loco-regional delivery to treat other relevant cancers (e.g., colon cancer, pancreatic cancer, and gastric cancer).

Till now, there have been several direct glycolysis-targeting agents tested both in preclinical and clinical stages as anti-tumor agents, with promising results [45-48]. In addition to these direct glycolysis-targeting agents, the data of our work point out that once an agent (e.g., Nano-Taxol) harbors the ability to indirectly switch glycolysis to OXPHOS, it also shows satisfactory tumor control.

In summary, in this translational research, we display that a novel nanoparticle-encapsulated paclitaxel (Nano-Taxol) shows dramatic anti-tumor efficacy in the treatment of ovarian cancer through intraperitoneal delivery (a type of loco-regional delivery). The anti-tumor efficacy shown by this mode of treatment performs better than the current standard treatment (intravenous delivery of Taxol®). This concept may be further extended to treat several relevant cancers that have been proved to suitable for loco-regional delivery of therapeutic agents (e.g., colon cancer, pancreatic cancer, and gastric cancer) in the future.

Acknowledgements

The authors thank the Genomics Research Centre and the National Yang Ming University for providing facilities and support for tumor imaging. This study was funded by in part by National Science Council, Taiwan (grant number NSC 103-NU-E-010-003-NU).

Disclosure of conflict of interest

None.

Abbreviations

GLUT1, glucose transporter 1; Cu/ZnSOD, copper/zinc superoxide dismutase; MnSOD, manganese superoxide dismutase; OXPHOS, oxidative phosphorylation; PT, parental cells; ROS, reactive oxygen species; TR, Taxol®-resistant cells.

Address correspondence to: Chi-Mu Chuang, Institute of Clinical Medicine, School of Medicine, National Yang-Ming University, No.155, Sec. 2, Linong Street, Taipei, 112 Taiwan (ROC). Tel: +886-2-2875-7826; Fax: +886-2-77232788; E-mail: cmjuang@gmail.com

References

- [1] Siddique HR and Saleem M. Role of BMI1, a stem cell factor, in cancer recurrence and chemoresistance: preclinical and clinical evidences. *Stem Cells* 2012; 30: 372-378.
- [2] Brabletz T. To differentiate or not—routes towards metastasis. *Nat Rev Cancer* 2012; 12: 425-436.
- [3] Barker N, Ridgway RA, van Es JH, van de Wetering M, Begthel H, van den Born M, Danenberg E, Clarke AR, Sansom OJ and Clevers H. Crypt stem cells as the cells-of-origin of intestinal cancer. *Nature* 2009; 457: 608-611.
- [4] Hjelmeland AB, Wu Q, Heddleston JM, Choudhary GS, MacSwords J, Lathia JD, McLendon R, Lindner D, Sloan A and Rich JN. Acidic stress promotes a glioma stem cell phenotype. *Cell Death Differ* 2011; 18: 829-840.
- [5] Samanta D, Gilkes DM, Chaturvedi P, Xiang L and Semenza GL. Hypoxia-inducible factors are required for chemotherapy resistance of breast cancer stem cells. *Proc Natl Acad Sci U S A* 2014; 111: E5429-5438.
- [6] Warburg O. On the origin of cancer cells. *Science* 1956; 123: 309-314.
- [7] Ye XQ, Wang GH, Huang GJ, Bian XW, Qian GS and Yu SC. Heterogeneity of mitochondrial membrane potential: a novel tool to isolate and identify cancer stem cells from a tumor mass? *Stem Cell Rev* 2011; 7: 153-160.
- [8] Shen YA, Wang CY, Hsieh YT, Chen YJ and Wei YH. Metabolic reprogramming orchestrates cancer stem cell properties in nasopharyngeal carcinoma. *Cell Cycle* 2015; 14: 86-98.
- [9] Jain RK and Stylianopoulos T. Delivering nanomedicine to solid tumors. *Nat Rev Clin Oncol* 2010; 7: 653-664.
- [10] Schroeder A, Heller DA, Winslow MM, Dahlman JE, Pratt GW, Langer R, Jacks T and Anderson DG. Treating metastatic cancer with nanotechnology. *Nat Rev Cancer* 2012; 12: 39-50.

Nano-Taxol can switch status of cancer metabolism

- [11] Kadam RS, Bourne DW and Kompella UB. Nano-advantage in enhanced drug delivery with biodegradable nanoparticles: contribution of reduced clearance. *Drug Metab Dispos* 2012; 40: 1380-1388.
- [12] Ferlay J, Soerjomataram I, Ervik M, Dikshit R, Eser S, Mathers C, Rebelo M, Parkin DM, Forman D, Bray F. GLOBOCAN 2012 v1.0, Cancer Incidence and Mortality Worldwide: IARC CancerBase No. 11. 2013. Available at: <http://globocan.iarc.fr>.
- [13] Institute NC. Cancer Stat Fact Sheets, The Surveillance, Epidemiology, and End Results (SEER) cancer statistics. 2014. Available at: <http://seer.cancer.gov/statfacts/html/ovary.html>.
- [14] Lu Z, Wang J, Wientjes MG and Au JL. Intraperitoneal therapy for peritoneal cancer. *Future Oncol* 2010; 6: 1625-1641.
- [15] Liu J and Matulonis UA. New strategies in ovarian cancer: translating the molecular complexity of ovarian cancer into treatment advances. *Clin Cancer Res* 2014; 20: 5150-5156.
- [16] Martins CP, Brown-Swigart L and Evan GI. Modeling the therapeutic efficacy of p53 restoration in tumors. *Cell* 2006; 127: 1323-1334.
- [17] Liu J and Matulonis UA. New strategies in ovarian cancer: translating the molecular complexity of ovarian cancer into treatment advances. *Clin Cancer Res* 2014; 20: 5150-5156.
- [18] Maeda H. Tumor-selective delivery of macromolecular drugs via the EPR effect: background and future prospects. *Bioconjug Chem* 2010; 21: 797-802.
- [19] Hector S, Rehm M, Schmid J, Kehoe J, McCawley N, Dicker P, Murray F, McNamara D, Kay EW, Concannon CG, Huber HJ and Prehn JH. Clinical application of a systems model of apoptosis execution for the prediction of colorectal cancer therapy responses and personalisation of therapy. *Gut* 2012; 61: 725-733.
- [20] Kano MR, Bae Y, Iwata C, Morishita Y, Yashiro M, Oka M, Fujii T, Komuro A, Kiyono K, Kaminishi M, Hirakawa K, Ouchi Y, Nishiyama N, Kataoka K and Miyazono K. Improvement of cancer-targeting therapy, using nanocarriers for intractable solid tumors by inhibition of TGF-beta signaling. *Proc Natl Acad Sci U S A* 2007; 104: 3460-3465.
- [21] Lammers T, Kiessling F, Hennink WE and Storm G. Drug targeting to tumors: principles, pitfalls and (pre-) clinical progress. *J Control Release* 2012; 161: 175-187.
- [22] Jacquet P and Sugarbaker PH. Peritoneal-plasma barrier. *Cancer Treat Res* 1996; 82: 53-63.
- [23] Soma D, Kitayama J, Konno T, Ishihara K, Yamada J, Kamei T, Ishigami H, Kaisaki S and Nagawa H. Intraperitoneal administration of paclitaxel solubilized with poly(2-methacryloxyethyl phosphorylcholine-co n-butyl methacrylate) for peritoneal dissemination of gastric cancer. *Cancer Sci* 2009; 100: 1979-1985.
- [24] Markman M, Brady MF, Spirtos NM, Hanjani P and Rubin SC. Phase II trial of intraperitoneal paclitaxel in carcinoma of the ovary, tube, and peritoneum: a Gynecologic Oncology Group Study. *J Clin Oncol* 1998; 16: 2620-2624.
- [25] Armstrong DK, Bundy B, Wenzel L, Huang HQ, Baergen R, Lele S, Copeland LJ, Walker JL, Burger RA; Gynecologic Oncology Group. Intraperitoneal cisplatin and paclitaxel in ovarian cancer. *N Engl J Med* 2006; 354: 34-43.
- [26] Sharma A, Sharma US and Straubinger RM. Paclitaxel-liposomes for intracavitary therapy of intraperitoneal P388 leukemia. *Cancer Lett* 1996; 107: 265-272.
- [27] Shukla D, Chakraborty S, Singh S and Mishra B. Lipid-based oral multiparticulate formulations - advantages, technological advances and industrial applications. *Expert Opin Drug Deliv* 2011; 8: 207-224.
- [28] Ait-Oudhia S, Mager DE and Straubinger RM. Application of pharmacokinetic and pharmacodynamic analysis to the development of liposomal formulations for oncology. *Pharmaceutics* 2014; 6: 137-174.
- [29] Feng W, Gentles A, Nair RV, Huang M, Lin Y, Lee CY, Cai S, Scheeren FA, Kuo AH and Diehn M. Targeting unique metabolic properties of breast tumor initiating cells. *Stem Cells* 2014; 32: 1734-1745.
- [30] Palorini R, Votta G, Balestrieri C, Monestiroli A, Olivieri S, Vento R and Chiaradonna F. Energy metabolism characterization of a novel cancer stem cell-like line 3AB-OS. *J Cell Biochem* 2014; 115: 368-379.
- [31] Gammon L, Biddle A, Heywood HK, Johannesen AC and Mackenzie IC. Sub-sets of cancer stem cells differ intrinsically in their patterns of oxygen metabolism. *PLoS One* 2013; 8: e62493.
- [32] Menendez JA, Joven J, Cufi S, Corominas-Faja B, Oliveras-Ferraro C, Cuyas E, Martin-Castillo B, Lopez-Bonet E, Alarcon T and Vazquez-Martin A. The Warburg effect version 2.0: metabolic reprogramming of cancer stem cells. *Cell Cycle* 2013; 12: 1166-1179.
- [33] Pecqueur C, Oliver L, Oizel K, Lalier L and Vallette FM. Targeting metabolism to induce cell death in cancer cells and cancer stem cells. *Int J Cell Biol* 2013; 2013: 805975.
- [34] Vander Heiden MG. Targeting cancer metabolism: a therapeutic window opens. *Nat Rev Drug Discov* 2011; 10: 671-684.
- [35] Vousden KH and Prives C. Blinded by the Light: The Growing Complexity of p53. *Cell* 2009; 137: 413-431.
- [36] Green DR and Chipuk JE. p53 and metabolism: Inside the TIGAR. *Cell* 2006; 126: 30-32.

Nano-Taxol can switch status of cancer metabolism

- [37] Schwartzberg-Bar-Yoseph F, Armoni M and Karnieli E. The tumor suppressor p53 down-regulates glucose transporters GLUT1 and GLUT4 gene expression. *Cancer Res* 2004; 64: 2627-2633.
- [38] Corcoran CA, Huang Y and Sheikh MS. The regulation of energy generating metabolic pathways by p53. *Cancer Biol Ther* 2006; 5: 1610-1613.
- [39] Assaily W and Benchimol S. Differential utilization of two ATP-generating pathways is regulated by p53. *Cancer Cell* 2006; 10: 4-6.
- [40] Suzuki S, Tanaka T, Poyurovsky MV, Nagano H, Mayama T, Ohkubo S, Lokshin M, Hosokawa H, Nakayama T, Suzuki Y, Sugano S, Sato E, Nagao T, Yokote K, Tatsuno I and Prives C. Phosphate-activated glutaminase (GLS2), a p53-inducible regulator of glutamine metabolism and reactive oxygen species. *Proc Natl Acad Sci U S A* 2010; 107: 7461-7466.
- [41] Kotala V, Uldrijan S, Horky M, Trbusek M, Strnad M and Vojtesek B. Potent induction of wild-type p53-dependent transcription in tumour cells by a synthetic inhibitor of cyclin-dependent kinases. *Cell Mol Life Sci* 2001; 58: 1333-1339.
- [42] Zawacka-Pankau J, Grinkevich VV, Hunten S, Nikulenkov F, Gluch A, Li H, Enge M, Kel A and Selivanova G. Inhibition of glycolytic enzymes mediated by pharmacologically activated p53: targeting Warburg effect to fight cancer. *J Biol Chem* 2011; 286: 41600-41615.
- [43] Dey A, Verma CS and Lane DP. Updates on p53: modulation of p53 degradation as a therapeutic approach. *Br J Cancer* 2008; 98: 4-8.
- [44] Glantz MJ, LaFollette S, Jaeckle KA, Shapiro W, Swinnen L, Rozental JR, Phuphanich S, Rogers LR, Gutheil JC, Batchelor T, Lyter D, Chamberlain M, Maria BL, Schiffer C, Bashir R, Thomas D, Cowens W and Howell SB. Randomized trial of a slow-release versus a standard formulation of cytarabine for the intrathecal treatment of lymphomatous meningitis. *J Clin Oncol* 1999; 17: 3110-3116.
- [45] Michelakis ED, Sutendra G, Dromparis P, Webster L, Haromy A, Niven E, Maguire C, Gammer TL, Mackey JR, Fulton D, Abdulkarim B, McMurtry MS and Petruk KC. Metabolic modulation of glioblastoma with dichloroacetate. *Sci Transl Med* 2010; 2: 31ra34.
- [46] Fantin VR, St-Pierre J and Leder P. Attenuation of LDH-A expression uncovers a link between glycolysis, mitochondrial physiology, and tumor maintenance. *Cancer Cell* 2006; 9: 425-434.
- [47] Le A, Cooper CR, Gouw AM, Dinavahi R, Maitra A, Deck LM, Royer RE, Vander Jagt DL, Semenza GL and Dang CV. Inhibition of lactate dehydrogenase A induces oxidative stress and inhibits tumor progression. *Proc Natl Acad Sci U S A* 2010; 107: 2037-2042.
- [48] Samudio I, Harmancey R, Fiegl M, Kantarjian H, Konopleva M, Korchin B, Kaluarachchi K, Bornmann W, Duvvuri S, Taegtmeier H and Andreeff M. Pharmacologic inhibition of fatty acid oxidation sensitizes human leukemia cells to apoptosis induction. *J Clin Invest* 2010; 120: 142-156.